

An ignition criterion for inertial fusion boosted by microturbulence



Cite as: Phys. Plasmas **33**, 020703 (2026); doi: 10.1063/5.0295335

Submitted: 8 August 2025 · Accepted: 10 January 2026 ·

Published Online: 10 February 2026



Henry Fetsch^{a)} and Nathaniel J. Fisch

AFFILIATIONS

Department of Astrophysical Sciences, Princeton University, Princeton, New Jersey 08544, USA

^{a)}Author to whom correspondence should be addressed: hfetsch@princeton.edu

ABSTRACT

Turbulence on fine spatial scales enhances fusion reactivity, enabling ignition at lower temperature. A modified Lawson-like ignition criterion is derived for inertially confined plasmas harboring turbulent kinetic energy. For some turbulent energy spectra, hot spots ignite at lower energy density and smaller volume. While detrimental mixing effects typically accompany turbulence and obscure these advantages, targets might be engineered to drive flow in regions where it is beneficial. The optimal length scale for this driving is identified, typically lying in the micrometer range.

© 2026 Author(s). All article content, except where otherwise noted, is licensed under a Creative Commons Attribution (CC BY) license (<https://creativecommons.org/licenses/by/4.0/>). <https://doi.org/10.1063/5.0295335>

Thermonuclear ignition requires that fuel be driven to high temperature and density and be adequately confined so that heating by fusion products exceeds energy losses. The classic Lawson criterion¹ quantifies this requirement. Inertial confinement fusion (ICF) comes with the complication that the hot fuel is typically disassembling even while igniting, thereby losing energy to mechanical work in addition to the radiation and transport present in magnetic confinement devices. The ICF community has therefore developed several generalized Lawson criteria (GLC) based on power balance,^{2–6} on other thermodynamic properties of the hot spot,^{7–9} or on related criteria such as the positivity of the second time-derivative of the temperature.² Alternatively, ignition may simply be defined as fusion gain exceeding unity.¹⁰ Maximizing gain requires that compression expend minimal energy per unit of fusion yield. Other than the necessary heating of fuel ions, any process that increases energy losses, reduces confinement time, or consumes compression energy therefore degrades gain. Residual kinetic energy (RKE), the portion of the implosion energy that remains in flows rather than thermalizing, is detrimental in all of these respects.^{11–16} Success in reducing RKE has contributed to improvements in ICF performance and to the achievement of ignition.^{8,10,17,18}

However, this is not the full story. As a fast ion travels through plasma containing small-scale turbulent fluctuations, its peculiar velocity varies with respect to the local fluid flows. A particle near the thermal bulk in one region can end up further out on the tail if it travels to another region with different flow. The result is a broadening of the

tail of the ion distribution and thus an enhancement to fusion reactivity.¹⁹ This recently identified shear flow reactivity enhancement effect (SFRE) can multiply reactivity severalfold under ICF-relevant conditions.^{19,20} Because fusion is driven by fast ions, whose mean free paths are much longer than those of the thermal particles that determine viscosity, a large reactivity enhancement is possible even when flow gradients are weak and viscous dissipation is slow. It follows that some turbulent kinetic energy (TKE) might, in fact, assist in ignition.

Such an advantage is not captured in the Lawson criterion^{1,4} $p\tau > F(T)$, which is agnostic of TKE (p is the pressure, τ is the confinement time, and F is a function of temperature T). Following the form of Betti *et al.*,⁴ who define a parameter χ such that ignition corresponds to $\chi > 1$, this Letter introduces a new GLC for turbulent plasma. The modified ignition parameter χ_{turb} accounts for the SFRE and is a functional of the hot-spot turbulent energy spectrum. Remarkably, TKE on short length scales can increase χ_{turb} more efficiently than thermal energy; TKE on longer scales is detrimental, as in the conventional picture. Some non-igniting targets would instead ignite if a portion of their energy were redirected into TKE. This class of implosions, characterized by $\chi_{\text{turb}} > 1 > \chi$, represents a new ICF regime enabled by turbulence.

We first consider ignition of a typical isobaric hot spot containing no turbulence, which is assumed for simplicity to be spherically symmetric. After stagnation, the hot spot expands against a surrounding shell of cold, dense fuel (left side of Fig. 1). Some alpha particles, radiation, and conducted heat escape the hot spot, but a portion of escaping

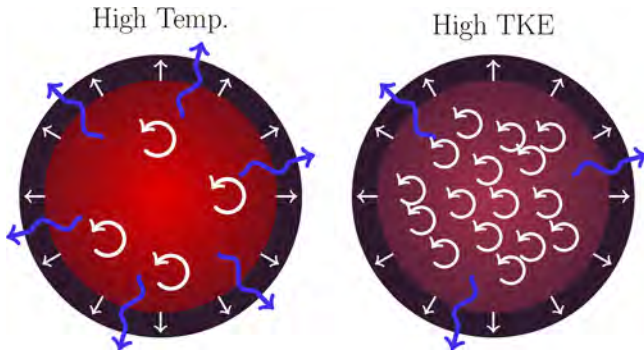


FIG. 1. Replacement of thermal energy with TKE. The left panel shows a conventional ICF hot spot (red) with little internal turbulence. On the right, some thermal energy is replaced with TKE. Both hot spots expand into the cold shell (gray), but the turbulent hot spot emits less radiation (blue arrows). The thermal reactivity of the turbulent hot spot is lower, but the turbulent enhancement can be large.

energy is recycled through ablation of cold fuel.^{4,5} Therefore, as an approximation, we neglect heat conduction.^{4,21} In deuterium-tritium (DT) plasma, the self-heating condition is

$$Q_\alpha > Q_b + Q_w, \quad (1)$$

where $Q_\alpha = f_\alpha p^2 \epsilon_\alpha S(T)$ is the power density due to alpha heating, $Q_b = f_b p^2 B(T)$ is the radiated power density, and $Q_w = p/\tau$ is the rate of mechanical work. Here, f_α is the fraction of fusion power deposited in the hot spot, f_b is the fraction of radiated power escaping the hot spot, and ϵ_α is the birth energy of alpha particles. In terms of the hot-spot central temperature T , the reactivity function $S(T)$ is defined as

$$S(T) = \frac{1}{V} \int_V d^3 r \frac{\langle \sigma v \rangle}{\tilde{T}^2}, \quad (2)$$

where $\langle \sigma v \rangle$ is the fusion reactivity, $\tilde{T}(r)$ is the spatially varying temperature, and V is the hot-spot volume. The pressure, which is taken to be uniform throughout the hot spot, is $p = 2nT$, where n is the ion number density. We follow previous authors³⁻⁵ in approximating S and B by power laws. With T in keV, the fit $S(T) \approx S_0 T^{\omega-2}$, with $S_0 \approx 2.78 \times 10^{-21} \text{ keV}^{-2} \text{ cm}^3 \text{ s}^{-1}$ and $\omega \approx 3.26$, is obtained in the region $4 \text{ keV} \leq T \leq 12 \text{ keV}$ using the temperature profile $\tilde{T}(r) \approx T(1 - r^2/R^2)^{2/5} / (1 - 0.15r^2/R^2)$ where R is the hot-spot radius.⁴ The fit $B(T) \approx B_0 T^{\beta-2}$, with $B_0 \approx 8.34 \times 10^{-16} \text{ keV}^{-1} \text{ cm}^3 \text{ s}^{-1}$ and $\beta \approx 1/2$, approximates the net radiation (emission minus re-absorption) as uniform.⁵ Then Eq. (1) yields the ignition condition $\chi > 1$, where

$$\chi = (f_\alpha \epsilon_\alpha S_0 T^{\omega-2} - f_b B_0 T^{\beta-2}) \tau p. \quad (3)$$

When $\chi > 0$, alpha heating exceeds radiative losses; such a plasma would ignite if it were not expanding. The minimum temperature T_{ign} for static ignition is

$$T_{\text{ign}} = \left(\frac{f_b B_0}{f_\alpha \epsilon_\alpha S_0} \right)^{\frac{1}{\omega-\beta}}, \quad (4)$$

[note that f_α and f_b can depend on temperature, so Eq. (4) is not necessarily an explicit formula for T_{ign}]. The confinement time can be

estimated⁴ as $\tau \approx C_E R / v_{\text{imp}}$, where v_{imp} is the implosion velocity and we take $C_E = 1$ for simplicity. When $\chi > 1$, alpha heating overcomes both radiative losses and expansion, so the plasma ignites. This work does not consider subsequent burn propagation, which occurs when χ is large.⁹

Missing from all ignition criteria to date is an accounting for the direct effect of turbulence on fusion reactivity, the SFRE introduced in Ref. 19. Crucially, ions near the Gamow peak, where fusion reactions are most likely to occur, have velocities much greater than the thermal velocity v_{th} . The mean free path of these fast ions is correspondingly much longer than the thermal mean free path λ_{th} . In turbulent plasma, where gradients may be weak on thermal-particle scales but strong on fast-particle scales, nonlocal kinetic modifications to the ion distribution function can significantly affect fusion reactivity. The SFRE is extremely expensive to capture numerically *ab initio*, requiring high-resolution viscous fluid simulations coupled to accurate fast-ion kinetic simulations. Instead, Ref. 20 derived an analytical formula for the SFRE in low Mach-number flows. Although this formula is generally an underestimate, it offers a useful quantitative model for the purposes of this Letter. Moreover, the restriction to low Mach number (flows much slower than v_{th}) leads to the elegant result that the enhancement factor is simply a functional of the turbulent energy spectrum. [When the flow field is decomposed into shear modes $\tilde{u}(k)$, the first nonzero correction to the reactivity is second order in \tilde{u} , and the only terms with a nonzero spatial average have the form $\tilde{u}(k)\tilde{u}(-k)$]. We are thus able to consider the effect of turbulence without prescribing its exact structure.

Suppose that some of the thermal energy of a fusion plasma is replaced with TKE. Holding the energy density and number density constant, the temperature must decrease, as sketched in Fig. 1. The flow is assumed to be isotropic and present only on scales smaller than the hot-spot radius. For simplicity, the flow is treated as divergence-free, although pressure fluctuations in compressible turbulence could produce a small additional enhancement. The thermal pressure is replaced by an effective pressure, which includes both thermal and turbulent contributions.²³ Let p and n take the same values as before, with p now denoting the effective pressure, and let θ be the ratio of TKE to thermal energy so that $p = 2nT(1 + \theta)$. The “effective temperature” is $T_{\text{eff}} = p/2n$ (absent turbulence, $T_{\text{eff}} = T$). If the turbulent flow field is decomposed into solenoidal modes on various length scales, the contribution to the reactivity from each mode increases with its wavenumber k . The reactivity is multiplied by an enhancement factor $\Phi \approx 1 + 2 \int dk E(k) G(k)$, where $E(k)$ is the turbulent energy spectrum and $G(k)$ is derived in Ref. 20. Figure 2(a) shows the DT, deuterium-deuterium (DD), and D³He reactivities²² in thermal plasma and in “turbulent” plasma modeled by a single shear mode. The TKE per ion is $T/2$, implying $\theta = 1/6$ for DT and DD, and $\theta = 2/15$ for equimolar D³He (because of its higher electron heat capacity). Two cases are shown: a turbulent Knudsen number of 0.1 and the limiting case of asymptotically large k . In Fig. 2(b), the alpha-heating power in equimolar DT plasma is compared to power radiated by bremsstrahlung in thermal ($\theta = 0$) and turbulent ($\theta = 1/6$) plasma, assuming $f_\alpha = f_b = 1$. Here, the horizontal axis shows T_{eff} , meaning that turbulence corresponds to lower T . Nevertheless, T_{ign} shifts lower due both to reactivity enhancement and to the decrease in radiation. Per Fig. 2(a), a similar shift occurs for other reactions, which could make ignition of D³He and DD plasmas more practical. However, the remainder of this Letter considers only DT ignition.

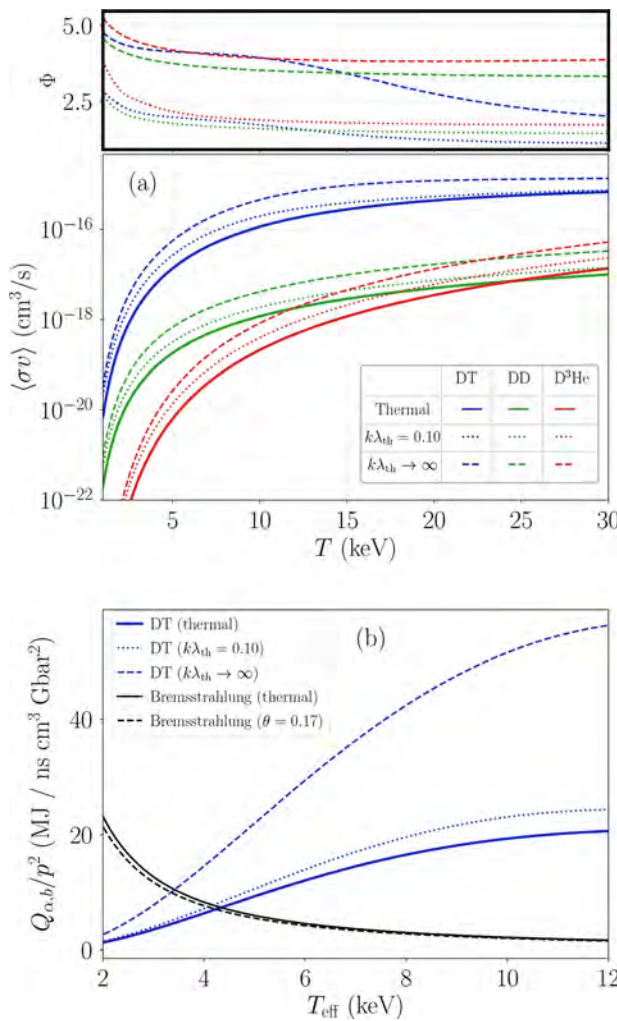


FIG. 2. (a) Thermal²² and turbulence-enhanced reactivities²⁰ for the DT [$\text{T}(\text{d},\text{n})^4\text{He}$], DD [$\text{D}(\text{d},\text{p})\text{T}$ and $\text{D}(\text{d},\text{n})^3\text{He}$], and D^3He [$^3\text{He}(\text{d},\text{p})^4\text{He}$] reactions. (Top panel: enhancement factor Φ). The turbulent energy is $\int_0^\infty dkE(k) = T/2$, meaning $\theta = 1/6$ for DD and DT and $\theta = 2/15$ for D^3He . (b) DT alpha heating compared to bremsstrahlung at temperatures relevant to ICF.

Accounting for the reactivity enhancement, the alpha-heating power can be written as $Q_\alpha = f_\alpha p^2 \epsilon_\alpha S(T)(1 + \theta H)$, where based on Ref. 20, we define

$$H = \int_0^\infty dk h(k) \frac{E(k)}{\int_0^\infty dk' E(k')}, \quad h(k) = \frac{T}{E(k)} \left\langle 6 \frac{\tilde{E}(k)G(k)}{\tilde{T}} \right\rangle_{\text{reac}}, \quad (5)$$

and the average is taken over the hot-spot volume weighted by the reaction rate. Note that $\theta = \int_0^\infty dkE(k)/3T$ for DT plasma. Here, $\tilde{E}(k, \mathbf{r})$ is the local spectrum such that $E(k) = \int_0^R dr 4\pi r^2 \tilde{E}(k, \mathbf{r})/V$. We approximate the distribution of TKE by the following simple model. Assume that all TKE is concentrated within some radius r_{max} , let the ratio of TKE to T be constant, and let the spectrum shift proportionally to the density $\tilde{n}(r) = p/2\tilde{T}(r)$ so that denser regions support finer-scale structures. In other words, $\tilde{E}(k, r_1) = \tilde{E}(k\tilde{T}(r_1)/\tilde{T}(r_2), r_2)$

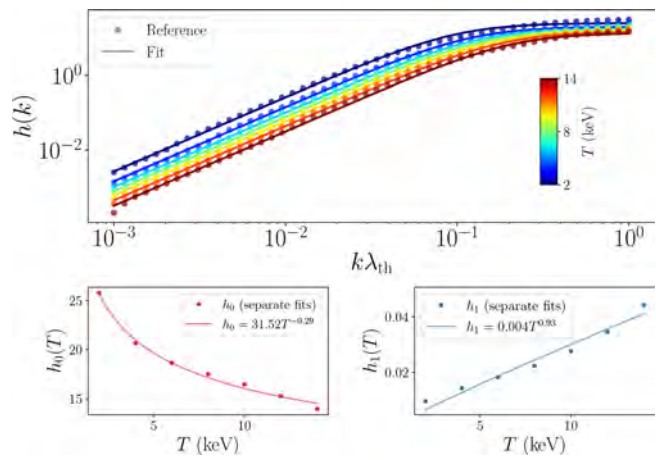


FIG. 3. Fit of $h(k)$ with parameters described in Eq. (6). Reference data generated from the “corrected utility function” of Ref. 20.

for radii $r_1, r_2 < r_{\text{max}}$. Using the $G(k)$ formula from Ref. 20 and fixing $r_{\text{max}} = 0.8R$ for simplicity, $h(k)$ was fit to the functional form

$$h(k) = h_0(T) \frac{(k\lambda_{\text{th}})^2}{(k\lambda_{\text{th}})^2 + h_1(T)}. \quad (6)$$

The parameters $h_0 \approx 31.52T^{-0.29}$ and $h_1 \approx 0.004T^{0.93}$, with T in keV, provide a good fit, as shown in Fig. 3.

Now, suppose that we introduce some turbulence into an ICF hot spot. The ignition condition becomes $\chi_{\text{turb}} > 1$, where the modified ignition parameter χ_{turb} is

$$\chi_{\text{turb}} = \left(\frac{f_\alpha \epsilon_\alpha S_0 T_{\text{eff}}^{\omega-2}}{(1+\theta)^\omega} (1 + \theta H) - \frac{f_b B_0 T_{\text{eff}}^{\beta-2}}{(1+\theta)^\beta} (1 + \theta M) \right) \tau p, \quad (7)$$

and M estimates the increase in emission due to turbulent mixing of high-Z material into the hot spot.^{11,24} Note that f_α and f_b may also vary with temperature and should be evaluated at $T = T_{\text{eff}}/(1+\theta)$. We take $f_b = 0.3$ and follow Ref. 2 to write

$$f_\alpha = \begin{cases} \frac{3}{2}\ell - \frac{4}{5}\ell^2, & \ell \leq 1/2, \\ 1 - \frac{1}{4\ell} + \frac{1}{160\ell^3}, & \ell > 1/2, \end{cases} \quad (8)$$

where $\ell = 66.7(T^{-1.25} + 0.0082)\rho R$ for ρR in g/cm^2 . To isolate the effect of the SFRE, we take $M = 0$. This does not imply that the mix level is necessarily zero; rather, it assumes that mix does not increase with the energy in the deliberately driven turbulence. This assumption is likely incompatible with turbulence driven by perturbations to the target surface,^{11,13,24} but it may be reasonable for turbulence driven by internal target structures and kept away from the boundary.

The modified ignition condition is displayed in Fig. 4 as contours in the space of hot-spot areal density ρR and effective temperature T_{eff} . Each curve corresponds to flows on a scale $L = R/m$, where m is a mode number and $k = 2\pi/L$. Apart from the physical significance of driving high-mode perturbations, contours conveniently then depend on ρR rather than on ρ or R individually. All cases shown

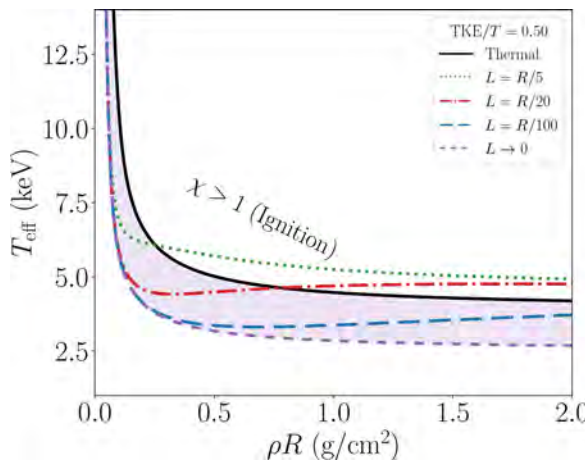


FIG. 4. Ignition contours $\chi_{\text{turb}} = 1$ for implosions with $v_{\text{imp}} = 400 \text{ km/s}$ and $C_E = 1$ and with varying shear length scales. Here, $\theta = 1/6$. The thermal case recovers the non-turbulent χ . In the shaded region, where $\chi_{\text{turb}} > 1 > \chi$, ignition requires the SFRE.

correspond to $\theta = 1/6$. With low-mode flows, ignition becomes easier in some regimes (low ρR , high T) and harder in others (high ρR , low T). The limiting $L \rightarrow 0$ case shows the maximum enhancement for $\theta = 1/6$, corresponding to the saturation of G at high k . In the shaded region, where $\chi_{\text{turb}} > 1 > \chi$, ignition is possible with $\theta = 1/6$ but impossible without turbulence. This is true for two reasons: First, the contour shifts downward when the SFRE exceeds the decrease in reactivity due to reducing T ; second, at low ρR , reducing T shortens the alpha-particle mean free path, permitting ignition of a smaller hot spot.¹⁹ In the already-igniting $\chi > 1$ regime, increased χ_{turb} implies faster ignition and higher yield.^{3,5,8,9}

Evidently, turbulence is beneficial on some scales and detrimental on others. A key question for ICF experiments is then the following: *If hot-spot thermal energy is exchanged for TKE with a spectrum $E(k)$, does the resulting system ignite more easily?*

In principle, this question can be answered precisely only by detailed simulations of specific experiments. However, one can seek a useful estimate by asking how χ_{turb} responds to a small amount of added TKE. Considering for simplicity perturbations about a turbulence-free state, the efficiency function $\psi_0(k)$ for driving energy into mode k is defined as

$$\psi_0(k) = \frac{1}{|\chi|} \left(\frac{\partial \chi_{\text{turb}}}{\partial \theta} \right)_{p, \rho, E(k') \propto \delta(k-k'), \theta=0}, \quad (9)$$

which, using Eq. (7), takes the following simple form:

$$\psi_0(k) = \text{sgn}(\chi) \left(\beta - \phi_b - M + \frac{h(k) - \omega + \phi_a + \beta - \phi_b - M}{1 - \left(\frac{T_{\text{ign}}}{T} \right)^{\omega - \phi_a - \beta + \phi_b}} \right), \quad (10)$$

where sgn takes the sign (-1 or 1) of its argument, and $\phi_{a/b} = -Td(\ln f_{a/b})/dT$. The behavior of $\psi_0(k, T)$ is shown in Fig. 5(a) in a hot spot with $\rho = 100 \text{ g/cm}^3$, $R = 50 \mu\text{m}$, and

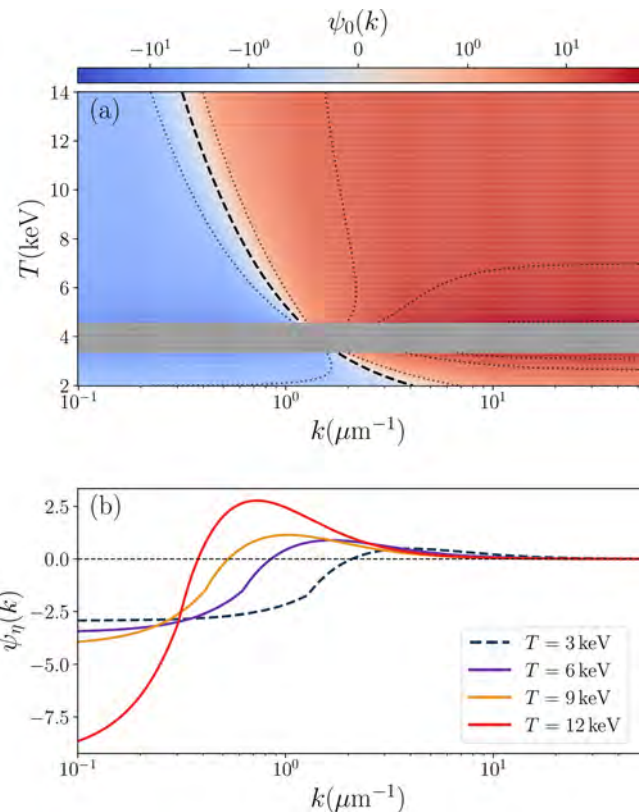


FIG. 5. (a) Efficiency functions for a range of temperatures and wavenumbers at $\rho = 100 \text{ g/cm}^3$, $R = 50 \mu\text{m}$, and $\tau = 50 \text{ ps}$. (a) ψ_0 (without viscosity). The region near $\chi = 0$ where Eq. (9) breaks down is shaded in gray. In addition to $\psi_0 = 0$, contours of $\psi_0 = \pm 1, 10, 20, 50$ are shown. (b) ψ_η for four values of T ; the 3 keV case is marked with a dashed line to highlight that $\chi < 0$. At the temperatures shown, the peak of ψ_η corresponds to approximately $k\lambda_\theta \approx 0.1$.

$\tau = 50 \text{ ps}$. To the right of the $\psi_0 = 0$ contour (black dashed line), exchanging some thermal energy for TKE is advantageous. This advantage increases dramatically with k on sub-micron scales, reaching values around $\psi_0 \approx 50$.

Viscosity becomes important on these short length scales, rapidly dissipating TKE.²⁵ Hence, the impact of TKE in high- k modes is damped because energy resides for a shorter time in these modes before being converted to thermal energy. As seen in Fig. 5(a), driven TKE has a larger effect at lower temperature. Rather than enhancing reactivity throughout the burn, the SFRE can be put to advantage by providing a “jump start” at early times, setting the hot spot on a more favorable ignition trajectory. The lifetime of driven turbulence should therefore be compared to the “ignition time” τ_{ign} , equal to $\tau/(\chi - 1)$ when $\chi > 2$ (otherwise $\tau_{\text{ign}} = \tau$). To quantify the effect of viscosity, we compute the dissipation time τ_η , viz.,

$$\tau_\eta = \frac{\left\langle \int_0^\infty dk \frac{\tilde{E}(k)G(k)}{\tilde{T}} \right\rangle_{\text{reac}}}{\left\langle \int_0^\infty dk 2\eta k^2 \frac{\tilde{E}(k)G(k)}{\tilde{T}} \right\rangle_{\text{reac}}}, \quad (11)$$

where η is the kinematic viscosity and τ_η is well approximated by $\tau_\eta \approx 793T^{-2.07}k^{-2}$ ps, with T in keV and k in μm^{-1} , for DT plasma at $\rho = 100 \text{ g/cm}^3$. We define a *viscous* efficiency function $\psi_\eta(k) = \min(1, \tau_\eta/\tau_{\text{ign}})\psi_0(k)$. This definition fails if the turbulent cascade carries TKE too quickly to smaller scales. However, in the regime of interest, the eddy turnover time is comparable to τ_η (for example, at $T = 6 \text{ keV}$, $\theta = 1/6$, and $k \sim 1 \mu\text{m}^{-1}$, both are approximately 20 ps). Hence, although inexact, τ_η gives a reasonable estimate of the TKE lifetime. Figure 5(b) shows $\psi_\eta(k)$ at several temperatures for the same parameters as in Fig. 5(a). Because of the k^{-2} dependence of τ_η , $\psi_\eta(k)$ has a peak at some $k_{\text{opt}}(T)$, representing the wavenumber at which TKE produces the largest time-averaged increase in χ_{turb} . Driving flows on length scales near $2\pi/k_{\text{opt}}$ represents a concrete design objective.

In practice, this driving could be accomplished using engineered defects in the target, possibly accompanied by adjustments to the drive profile. While such a design is beyond the scope of this Letter, we reference here some theoretical and experimental work supporting the feasibility of controlling ICF turbulence. Short-wavelength perturbations on the inner DT ice shell of a cryogenic target become Rayleigh–Taylor unstable during deceleration, generating flows;^{21,26} in fact, vorticity is seen to increase close to bang time,^{25,27–29} demonstrating that flows can affect the burn without being present (and subject to viscosity) throughout the implosion duration. Vortex structures formed in the hot spot, and the point of transition to turbulence, depend on the shell material,²⁷ indicating some degree of control. However, instabilities at the surface introduce mix that substantially degrades performance.^{11,13,24} Hence, while surface perturbations are easiest to control, mix means that the net effect of such perturbations is unlikely to be positive. A promising alternative is to drive turbulence in the interior of the hot spot using structured materials, such as wetted foams.^{30–33} Notably, ion kinetic effects, including a brief reactivity enhancement, appear during the collapse of voids in compressing foams,³⁴ suggesting that present experimental capabilities are suited to probing the regimes considered in this Letter, although fine control over the driven flows will require substantial further development. Fast ignition and shock ignition schemes,^{35–38} where fuel is compressed at low temperature and then rapidly heated, are particularly well suited to take advantage of the SFRE because viscosity remains low during compression then increases during heating (cf. the “sudden viscous dissipation” effect^{23,39,40}). Moreover, reducing the ignition temperature significantly relaxes energy requirements in these schemes.^{19,41,42}

This Letter generalizes the Lawson criterion to compressing turbulent plasma, independent of any particular ICF design. The modified criterion, $\chi_{\text{turb}} > 1$, reveals a new ICF regime (Fig. 4) where ignition is only possible by driving small-scale turbulence. These results apply to unmagnetized inertially confined plasma, but qualitatively similar effects may appear in magnetic confinement fusion devices. We employed a 1D hot-spot model to focus on the new physics of the SFRE, but the conclusions generalize readily to more complex, asymmetric hot spots; in fact, the efficiency functions ψ_0 and ψ_η are agnostic of hot-spot geometry. Thus, while quantitative refinements to χ_{turb} might be proposed for specific systems, the present results elucidate fundamental consequences of the partition between thermal and turbulent energy in ICF plasma.

This work was supported by the Center for Magnetic Acceleration, Compression, and Heating (MACH), part of the U.S. DOE-NNSA Stewardship Science Academic Alliances Program under Cooperative Agreement No. DE-NA0004148.

AUTHOR DECLARATIONS

Conflict of Interest

The authors have no conflicts to disclose.

Author Contributions

Henry Fetsch: Conceptualization (equal); Formal analysis (equal); Investigation (equal); Methodology (equal); Software (equal); Visualization (equal); Writing – original draft (equal); Writing – review & editing (equal). **Nathaniel J. Fisch:** Conceptualization (equal); Funding acquisition (equal); Project administration (equal); Resources (equal); Supervision (equal); Writing – review & editing (equal).

DATA AVAILABILITY

The data that support the findings of this study are available from the corresponding author upon reasonable request.

REFERENCES

- 1J. D. Lawson, *Proc. Phys. Soc., London, Sect. B* **70**, 6 (1957).
- 2J. D. Lindl, S. W. Haan, O. L. Landen, A. R. Christopherson, and R. Betti, *Phys. Plasmas* **25**, 122704 (2018).
- 3C. D. Zhou and R. Betti, *Phys. Plasmas* **15**, 102707 (2008).
- 4R. Betti, P. Y. Chang, B. K. Spears, K. S. Anderson, J. Edwards, M. Fatenejad, J. D. Lindl, R. L. McCrory, R. Nora, and D. Shvarts, *Phys. Plasmas* **17**, 058102 (2010).
- 5A. R. Christopherson, R. Betti, A. Bose, J. Howard, K. M. Woo, E. M. Campbell, J. Sanz, and B. K. Spears, *Phys. Plasmas* **25**, 012703 (2018).
- 6A. B. Zylstra, A. L. Kratcher, O. A. Hurricane, D. A. Callahan, J. E. Ralph, D. T. Casey, A. Pak, O. L. Landen, B. Bachmann, K. L. Baker *et al.*, *Phys. Rev. E* **106**, 025202 (2022).
- 7O. A. Hurricane, S. A. Maclare, M. D. Rosen, J. H. Hammer, P. T. Springer, and R. Betti, *Phys. Plasmas* **28**, 022704 (2021).
- 8O. A. Hurricane, A. Allen, B. L. Bachmann, K. L. Baker, S. Baxamusa, S. D. Bhandarkar, J. Biener, S. R. M. Bionta, T. Braun, T. Briggs *et al.*, *Plasma Phys. Controlled Fusion* **67**, 015019 (2025).
- 9A. R. Christopherson, R. Betti, S. Miller, V. Gopalaswamy, O. M. Mannion, and D. Cao, *Phys. Plasmas* **27**, 052708 (2020).
- 10H. Abu-Shwareb, R. Acree, P. Adams, J. Adams, B. Addis, R. Aden, P. Adrian, B. B. Afeyan, M. Aggleton, L. Aghaian *et al.*, *Phys. Rev. Lett.* **132**, 65102 (2024).
- 11A. Pak, L. Divol, C. Weber, L. B. Hopkins, D. Clark, E. Dewald, D. Fittinghoff, V. Geppert-Kleinrath, M. Hohenberger, S. Le Pape, T. Ma, A. MacPhee, D. Mariscal, E. Marley, A. Moore, L. Pickworth, P. Volegov, C. Wilde, O. Hurricane, and P. Patel, *Phys. Rev. Lett.* **124**, 145001 (2020).
- 12P. Springer, O. Hurricane, J. Hammer, R. Betti, D. Callahan, E. Campbell, D. Casey, C. Cerjan, D. Cao, E. Dewald *et al.*, *Nucl. Fusion* **59**, 032009 (2019).
- 13D. Patel, J. Knauer, D. Cao, R. Betti, R. Nora, A. Shvydky, V. Gopalaswamy, A. Lees, S. Sampat, W. Donaldson *et al.*, *Phys. Rev. Lett.* **131**, 105101 (2023).
- 14K. M. Woo, R. Betti, D. Shvarts, A. Bose, D. Patel, R. Yan, P.-Y. Chang, O. M. Mannion, R. Epstein, J. A. Delettrez *et al.*, *Phys. Plasmas* **25**, 052704 (2018).
- 15K. M. Woo, R. Betti, O. M. Mannion, C. J. Forrest, J. P. Knauer, V. N. Goncharov, P. B. Radha, D. Patel, V. Gopalaswamy, and V. Y. Glebov, *Phys. Plasmas* **27**, 062702 (2020).
- 16K. Churnetski, K. M. Woo, W. Theobald, R. Betti, L. Ceurvorst, C. J. Forrest, V. Gopalaswamy, P. V. Heuer, S. T. Ivancic, J. P. Knauer *et al.*, *Phys. Plasmas* **32**, 052711 (2025).

¹⁷A. L. Kritch, A. B. Zylstra, C. R. Weber, O. A. Hurricane, D. A. Callahan, D. S. Clark, L. Divol, D. E. Hinkel, K. Humbird, O. Jones *et al.*, *Phys. Rev. E* **109**, 025204 (2024).

¹⁸M. D. Rosen, *Phys. Plasmas* **31**, 090501 (2024).

¹⁹H. Fetsch and N. J. Fisch, *Phys. Rev. Lett.* **135**, 155101 (2025).

²⁰H. Fetsch and N. J. Fisch, *Phys. Plasmas* **32**, 112703 (2025).

²¹A. Bose, K. M. Woo, R. Nora, and R. Betti, *Phys. Plasmas* **22**, 072702 (2015).

²²H.-S. Bosch and G. M. Hale, *Nucl. Fusion* **32**, 611 (1992).

²³S. Davidovits and N. J. Fisch, *Phys. Plasmas* **26**, 062709 (2019).

²⁴P. K. Patel, P. T. Springer, C. R. Weber, L. C. Jarrott, O. A. Hurricane, B. Bachmann, K. L. Baker, L. F. Berzak Hopkins, D. A. Callahan, D. T. Casey *et al.*, *Phys. Plasmas* **27**, 050901 (2020).

²⁵C. R. Weber, D. S. Clark, A. W. Cook, L. E. Busby, and H. F. Robey, *Phys. Rev. E* **89**, 053106 (2014).

²⁶S. C. Miller and V. N. Goncharov, *Phys. Plasmas* **29**, 082701 (2022).

²⁷F. F. Grinstein, V. P. Chiravalle, B. M. Haines, R. K. Greene, and F. S. Pereira, *Flow, Turbul. Combust.* **114**, 801 (2025).

²⁸C. R. Weber, D. S. Clark, A. W. Cook, D. C. Eder, S. W. Haan, B. A. Hammel, D. E. Hinkel, O. S. Jones, M. M. Marinak, J. L. Milovich, P. K. Patel, H. F. Robey, J. D. Salmonson, S. M. Sepke, and C. A. Thomas, *Phys. Plasmas* **22**, 032702 (2015).

²⁹D. S. Clark, M. M. Marinak, C. R. Weber, D. C. Eder, S. W. Haan, B. A. Hammel, D. E. Hinkel, O. S. Jones, J. L. Milovich, P. K. Patel, H. F. Robey, J. D. Salmonson, S. M. Sepke, and C. A. Thomas, *Phys. Plasmas* **22**, 022703 (2015).

³⁰S. Davidovits, C. Federrath, R. Teyssier, K. S. Raman, D. C. Collins, and S. R. Nagel, *Phys. Rev. E* **105**, 065206 (2022).

³¹T. J. Murphy, B. J. Albright, M. R. Douglas, T. Cardenas, J. H. Cooley, T. H. Day, N. A. Denissen, R. A. Gore, M. A. Gunderson, J. R. Haack *et al.*, *High Energy Density Phys.* **38**, 100929 (2021).

³²B. J. Albright, T. J. Murphy, B. M. Haines, M. R. Douglas, J. H. Cooley, T. H. Day, N. A. Denissen, C. Di Stefano, P. Donovan, S. L. Edwards, J. Fincke *et al.*, *Phys. Plasmas* **29**, 022702 (2022).

³³B. M. Haines, T. J. Murphy, R. E. Olson, Y. Kim, B. J. Albright, B. Appelbe, T. H. Day, M. A. Gunderson, C. E. Hamilton, T. Morrow, and B. M. Patterson, *Phys. Plasmas* **30**, 072705 (2023).

³⁴L. Yin, B. J. Albright, E. L. Vold, W. D. Nystrom, R. F. Bird, and K. J. Bowers, *Phys. Plasmas* **26**, 062302 (2019).

³⁵M. Tabak, J. Hammer, M. E. Glinsky, W. L. Kruer, S. C. Wilks, J. Woodworth, E. M. Campbell, M. D. Perry, and R. J. Mason, *Phys. Plasmas* **1**, 1626–1634 (1994).

³⁶D. Clark and M. Tabak, *Nucl. Fusion* **47**, 1147–1156 (2007).

³⁷R. Betti, C. D. Zhou, K. S. Anderson, L. J. Perkins, W. Theobald, and A. A. Solodov, *Phys. Rev. Lett.* **98**, 155001 (2007).

³⁸L. J. Perkins, R. Betti, K. N. LaFortune, and W. H. Williams, *Phys. Rev. Lett.* **103**, 045004 (2009).

³⁹S. Davidovits and N. J. Fisch, *Phys. Rev. Lett.* **116**, 105004 (2016).

⁴⁰S. Davidovits and N. J. Fisch, *Phys. Rev. E* **94**, 053206 (2016).

⁴¹H. Fetsch and N. J. Fisch, *Phys. Rev. E* **108**, 045206 (2023).

⁴²A. R. Piriz and M. M. Sánchez, *Phys. Plasmas* **5**, 2721–2726 (1998).